On-line Supplementary Information

Moisture activation and carbon use efficiency of soil microbial communities along an aridity gradient in the Atacama Desert

Davey L. Jones, Sara Olivera-Ardid, Erwin Klumpp, Claudia Knief, Paul W. Hill, Eva Lehndorff, Roland Bol

S1. Additional site information

S1.1. Yungay (hyper-arid site)

Yungay is probably the most frequently studied region within the hyper-arid core of the Atacama Desert (1020 m above sea level; 24°8'54.67"S, 70°7'32.48"W). It receives < 2 mm rain per year and has a mean annual temperature of 14-16 °C with a maximum of 37.9 °C and minimum of -5.7 °C (Warren-Rhodes et al., 2006; McKay et al., 2003). The rainfall events may leave free water in the soil for ca. 3 d while it takes 10 d for the soil water content to revert back to pre-rainfall conditions (McKay et al., 2003). The relative humidity of the air at the site can vary from 1 to 95% depending on the presence of atmospheric fogs (Cáceres et al., 2007; Vitek et al., 2010; Wierzchos et al., 2015). Its hyper-aridity is not solely due to a lack of rainfall, however, but is also related to the very high potential evapotranspiration within the region (Wierzchos et al., 2015). In addition to its extreme aridity, the Atacama Desert holds the records for the highest surface UV radiation and total solar irradiances ever measured on Earth (Cordero et al., 2014; Rondanelli et al., 2015). Soil samples were taken from an alluvial fan with an age of around 2.1 Ma (Ewing et al., 2006). The landform originated from granitic source rocks and is covered by sparse desert pavement, which rests on a soil with atmospherically derived salts and dust (Fig. S1). The soil morphology and geochemistry for the site are described in detail in Ewing et al. (2006), Ewing et al. (2008) and Fletcher et al.

(2012). The site is devoid of any higher plants although lichens and microbial autotrophs are present (Patzelt et al., 2014). The taxonomy of the microbial communities determined by high through throughput sequencing can be found in Robinson et al. (2015).

Fig. S1. Photograph of the landscape at Yungay.

S1.2. Aroma (arid and hyper-arid sites)

The arid to hyper-arid transect at Aroma (1340 m above sea level, 19°46'53.1"S, 69°40'02.4"W to 2720 m; 19°31'42.7"S, 69°22'43.2"W) is located on the central part of a planation surface, formed 14.6 Ma ago on alluvial gravels (Evenstar et al., 2009). The surface comprises gravels that overlie Oligo-Miocene sediments and Paleocene and older igneous rocks. It has a well-developed desert pavement (Fig. S2; Evenstar et al., 2009). The supply of water (i.e. fogs, rainfall) at the Aroma transects stems from north-easterly (monsoonal) airflows that bring convective precipitation from Amazonia during the austral summer (Garreaud et al., 2003). A marked decrease in precipitation is observed with decreasing elevation (Houston and Hartley, 2003).

Fig. S2. Photographs showing the landscape at the hyper-arid (1340 m; left hand panel) and arid (2720 m; right hand panel) zones of the Aroma transect.

S1.3. Paposo (semi-arid site)

Samples at Paposo (25°00'43.02"S, 70°26'47.50"W) were collected at an elevation of ca. 570 m above sea level which is within the central fog zone (Fig. S3). The site has a sparse vegetation cover which comprises a diverse array of plant species as detailed in Rundel and Mahu (1976), Rundel (1978), Rundel et al. (1991) and Ehleringer et al. (1998). The species of highest abundance include *Euphorbia lactiflua*, *Lycopersicon chilense*, *Schizanthus laetus*, *Alstroemeria violacea* and *Chaetanthera glabrata*. Mean annual precipitation estimates are < 7 mm y^{-1} (Quade et al., 2007), however, the Loma vegetation at Paposo obtains a large proportion of its water from fog interception which is very frequent (Garreaud et al., 2008; Rundel et al., 1991). The relative humidity during these, often diurnal, fog events ranges from 70-90% (Rundel et al., 1991). Mean annual temperature at the site varies between 17 and 18 °C, and the parent material of the soils is derived from alluvial clasts and volcanic granite (Quade et al., 2007).

Fig. S3. Photographs showing the landscape at Paposo.

S2. Chemical characteristics of the soil in each moisture zone

The major properties of the surface soil profile from each aridity zone (hyper-arid, arid, and semi-arid) are shown in Table S1. Overall, all the soils were alkaline and most contained small amounts of mineral carbonates. The organic C content was low in both the hyper-arid and arid sites but was higher in the semi-arid sites, presumably due to the greater above- and below-ground inputs of C from higher plants growing within this region (Rundel et al., 1991). As expected, the total amount of N was also low at all sites. It should be noted, however, that the C:N ratios were low across all samples, indicating that C rather than N availability is limiting biological activity (Table S1). The inorganic pool was dominated by nitrate with concentrations similar to those measured previously within the region (Wang et al., 2016). The low amounts of NH_4^+ present (data not presented) are probably a result of the high pH, low moisture content and moderate temperatures that will drive NH_4^+ to be volatilized as NH_3 (Aggarwal and Praveenkumar, 1994). Even though total soil N was relatively low across the sites, the levels of NO_3^- and available P indicate that the microbial community is probably not N and P limited. Further, the available N:P ratios in the soil were also low across all the samples (mean ± SEM,

6.2 ± 3.3; n = 9) suggesting that these were stoichiometrically balanced from a microbial growth perspective (Vrede et al., 2002). Further work would be required to assess the microbial availability of different P forms in these soils. Metagenomic evidence suggests that the microbial community has the ability to assimilate both NH_4^+ and NO_3^- (Lynch et al., 2104; Davila et al., 2015). The results are also consistent with the accumulation of salts in these soils and the formation of minerals such as nitratite, halite, gypsum, anhydrite and calcite, particularly in the hyper-arid soils (Sutter et al., 2007). Further details of the soils and their physical and chemical properties can also be found in the references detailed in Section S1 above.

In the glucose addition experiment, we added the ^{14}C-labelled substrate to the soil at a rate of 72 g C kg^{-1}. Using the glucose-C, NO_3-N and Olsen-P data presented in Table S1, we calculated the 'available' C-to-N and C-to-P ratios for the hyper-arid site (where mineralization was most limited). On average, the C-to-N ratio was 1.4 ± 0.7 and the C-to-P ratio was 14.9 ± 2.7. These suggests that neither N or P were probably limiting microbial growth although more work would be required to validate this. In this respect, the biggest uncertainty lies in the Olsen-P values and the link between microbial P availability and Olsen-P values.

Table S1. Major characteristics of the surface soil profiles for the three different types of soils (semi-arid, arid and hyper-arid) used in the experiments. Values represent means. EC indicates electrical conductivity.

Aridity level	Depth (cm)	pH	EC ($\mu S\ cm^{-1}$)	Organic C	$CaCO_3$	Total N	C-to-N ratio	NO_3-N	Olsen-P
				(g kg^{-1} soil)				(mg kg^{-1} soil)	
Hyper-arid	0-1	7.70	554	0.37	5.7	0.15	2.47	25.8	6.7
	1-5	8.01	1106	0.33	8.6	0.16	2.06	76.5	3.6
	5-10	8.24	1775	0.31	5.7	0.27	1.15	136.6	5.2
Arid	0-1	7.59	26	0.56	<0.1	0.15	3.73	0.5	6.0
	1-5	8.13	27	0.87	<0.1	0.19	4.58	1.1	4.4
	5-10	8.50	25	0.88	2.0	0.23	3.83	0.6	3.8
Semi-arid	0-1	8.60	569	2.53	1.2	0.28	9.04	46.9	44.4
	1-5	8.83	455	2.86	0.2	0.23	12.4	37.3	28.3
	5-10	9.04	96	1.42	<0.1	0.11	12.9	6.6	3.7

S3. Choice of C substrates for use in the experiments

S3.1. Glucose as a C substrate

Glucose was chosen as a model C compound for our study as it can be taken up and used by almost all soil microorganisms. In addition, being neutrally charged, glucose does not bind to the soil's solid phase and can therefore be recovered from soil with a simple salt extract, thereby allowing us to estimate the amount of ^{14}C-glucose not taken up by the soil microbial community at the end of the experiment (Kuzyakov and Jones, 2008). There is also a precedent for using glucose to study microbial life in soils from the Atacama Desert (e.g. Quinn et al., 2007; Barros et al., 2008). The level of C substrate addition (10 mM; 72 mg C kg^{-1}) was chosen to reflect the likely concentration in soil following the lysis of a root or microbial cell (Jones and Darrah, 1996; Teusink et al., 1998; Bennet et al., 2009). This level of soluble C addition is higher than the soluble organic C measured in the soils used here (mean ± SEM in the hyper-arid sites = 0.45 ± 0.07 mg C kg^{-1}, arid sites = 0.86 ± 0.19 mg C kg^{-1}, semi-arid = 42.6 ± 14.1 mg C kg^{-1}) when measured with a 0.5 M K_2SO_4 extract (1:5 w/v) according to the method of Jones and Willett (2006). The amount added should therefore be enough to promote microbial growth, especially in the hyper-arid soils where the microbial biomass is extremely low. The ^{14}C-glucose was labelled at all six C positions (222 MBq $mmol^{-1}$; 39.96 GBq mg^{-1}) and was obtained from American Radiolabelled Chemicals Inc., St Louis, MO, USA.

S3.2. Plant material as a C substrate

Although perennial ryegrass (*Lolium perenne* L.) grows at lower altitudes in Chile (Campillo et al., 2005; Acuna et al., 2017), we acknowledge that it does not grow in the Atacama Desert. However, we chose this plant as it was readily available, was well characterised and contains all the high MW C polymers typically present in most plants (i.e. cellulose, hemicellulose, lignin, lipids and protein). To characterise the ^{14}C label in the plant leaf material, a sequential

chemical fractionation was performed according to Jones and Darrah (1994). Briefly, 50 mg of finely ground plant material was sequentially extracted in 8 ml deionised water for 30 min at 85°C, 8 ml 20% ethanol for 30 min at 80ºC, 5 ml 0.3% HCl for 3 h at 95ºC and 5 ml 1 M NaOH for 1 h at 95ºC. After each extraction step, the sample was centrifuged (5000 *g*, 15 min), the supernatant removed and its ^{14}C content determined using Optiphase 3® scintillation fluid (PerkinElmer, Waltham, MA) and a Wallac 1404 Liquid Scintillation Counter (PerkinElmer Corp.). Of the total ^{14}C contained in the plant material and subsequently added to soil, 32.9 ± 1.5% was extractable by water, 4.2 ± 0.2% by ethanol, 16.8 ± 0.6% by HCl, 27.5 ± 0.4% by NaOH and 18.5 ± 2.2% was insoluble residue. These components approximately correspond to readily decomposable or neutral-detergent soluble C (water and ethanol soluble), cellulose and hemicellulose (HCl soluble) and lignin (NaOH soluble and insoluble-humus) fractions of organic matter respectively (Domisch et al., 1998; Ekschmitt et al., 2008; Moorhead and Sinsabaugh, 2006). Prior to addition to the soil, the dry plant leaf material was ground to pass 1 mm to ensure that the material would become well mixed when added to the soil matrix. It should be noted that the amount of glucose-C and plant-derived-C were not equal and therefore the relative rates of $^{14}CO_2$ production for each substrate are not directly comparable.

S4. Calculation of microbial C use efficiency following the assimilation of glucose-C

The incubation period used here was sufficient to allow calculation of the relative amount of C partitioned into microbial anabolic processes (i.e. cell growth and maintenance) and the amount of C partitioned into catabolic processes (i.e. respiration). Microbial immobilization of the ^{14}C-substrate ($^{14}C_{imm}$) at the end of the incubation period was estimated as follows:

$$^{14}C_{imm} = {}^{14}C_{tot} - {}^{14}C_{NaCl} - {}^{14}CO_2 \qquad \text{(Eqn. 1)}$$

where $^{14}C_{tot}$ is the total amount of ^{14}C-substrate added to the soil at time (t) = 0, $^{14}C_{NaCl}$ is the amount of ^{14}C recovered in the 0.5 M NaCl extract and $^{14}CO_2$ is the total amount of ^{14}C

recovered as $^{14}CO_2$. Microbial C-substrate use efficiency (*CUE*) for each compound was then estimated as follows:

$$CUE = {}^{14}C_{imm} / ({}^{14}C_{imm} + {}^{14}CO_2) \quad \text{(Eqn. 2)}$$

The best estimates of *CUE* could be made for the wet soil treatments where a large proportion of the ^{14}C-glucose had been removed from solution at the end of the incubation period. In the humid and hyper-dry soil treatments, there was insufficient use of glucose to allow us to determine *CUE* with any confidence. Consequently, we only present *CUE* values for the wet-glucose treatment. It should be noted that the *CUE* values are only for the C within the glucose (i.e. substrate C use efficiency) and does not account for other C compounds also used by the biomass.

Another approach to estimating *CUE* is the modelling approach described in Glanville et al. (2016). This methodology is particularly suited to low molecular weight substrates such as glucose and uses a double exponential kinetic model to estimate ^{14}C partitioning into anabolic and catabolic microbial processes using the equation:

$$^{14}C_{loss} = (Pool_1 \times \exp^{-k_1 * t}) + (Pool_2 \times \exp^{-k_2 * t})$$

where, $^{14}C_{soil}$ is the amount of ^{14}C remaining in the soil over time (t), while a_1 and a_2 describe the size of each respective pool and k_1 and k_2 correspond to the exponential decay constants for each mineralization phase. Here, the first pool ($Pool_1$) corresponds to a C pool which is rapidly used for catabolic processes. The second, more recalcitrant pool ($Pool_2$) constitutes the remaining C immobilized within the microbial biomass (i.e. used for cell growth and maintenance, and ultimately necromass turnover). From this, CUE can be calculated as follows:

$$CUE = Pool_2 / (Pool_1 + Pool_2)$$

This approach is well suited to low molecular weight substrates which can rapidly cycle through the microbial biomass (such as glucose in soil held under wet conditions). Using the data presented for the treatment involving glucose addition in the wet soil we used the Glanville

et al. (2016) kinetic approach to calculate *CUE*. Overall, the model fitted well to the experimental data, particularly for the semi-arid and arid soils (Table S2). Based on the modelling parameters. In addition, our estimates of *CUE* showed the same trend as described in Figure 2 in the main paper.

Table S2. Kinetic parameters describing the turnover of ^{14}C-labelled glucose in the three different soil types (semi-arid, arid, hyper-arid) under the wet moisture regime.

	Modelled kinetic parameter				Model fit	CUE
	$Pool_1$ (%)	k_1 (d^{-1})	$Pool_2$ (%)	k_2 (d^{-1})	r^2	
Semi-arid	41.1	1.51	58.8	0.0089	0.999	0.588
Arid	25.8	0.41	74.3	0.0034	0.999	0.742
Hyper-arid	11.3	0.05	88.9	<0.0001	0.991	0.887

C use efficiency cannot be calculated for the ^{14}C-plant material as it was impossible to distinguish between ^{14}C held in the soil microbial biomass from that still remaining in the added ^{14}C-labelled plant material (at the end of the incubation period).

S5.1. Managing water activity in the treatments

S5.1. Use of Drierite® as a regulator of water activity in the hyper-dry experimental treatments

Driertite® is made from the naturally occurring mineral, gypsum ($CaSO_4$) and when absorbs water it creates calcium sulphate hemihydrate ($Ca_2H_2O_9S_2$). Many of the surface soils of the Atacama Desert contain abundant amounts of gypsum which maintains the soils at a low relative humidity but also represents a habitat for lithobiontic micro-organisms (Berger and Cooke, 1997; Cockell et al., 2008; Wierzchos et al., 2011). Drierite® is frequently used to maintain low and stable water activities within experiments (Reis et al., 2009; Faria et al., 2012). The amount we added was sufficient to ensure that the Drierite® did not become water saturated. The Drierite® maintains the relative humidity of the air above the soil at between

2.8-5.0%. This was confirmed in our samples with a HI9564 Thermohygrometer (Hanna Instruments Inc., Woonsocket, RI, USA). It should be noted that this value is below the water activity required for life (i.e. metabolic activity) in most environments (>60% relative humidity; Grant, 2004). At the hyper-arid site the relative humidity is below this 60% target value for 88% of the year (Wierzchos et al., 2011).

S5.2. Use of NaOH as a regulator of water activity in the humid/wet experimental treatments

For the humid treatment, a vial of NaOH (1 M) was included in the polypropylene container containing the soil. From a theoretical perspective, this should create a headspace atmosphere with a water activity of ca. 0.95 (i.e. 95% relative humidity) (An et al., 2014; Agnew et al., 2012). Our actual measurements indicated that the water activity was consistently >0.8. In the wet soil treatments, water was added to the soil and 1 M NaOH was present. In this case measurements of water activity in the headspace were >0.85. For reference, the relative humidity in the laboratory was ca. 70%.

S6. Supporting information to the results presented in the main text

S6.1. Amount of ^{14}C-glucose remaining in the soil at the end of the incubation period

The amount of ^{14}C-glucose remaining in the soil at the end of the incubation period was estimated with a 0.5 M NaCl extract. The biggest range in the amount of recoverable ^{14}C-glucose was seen in the wet moisture treatment where it ranged from 1.4 to 98.4% of the ^{14}C-glucose added to the soil. The amount of ^{14}C left in soil was also highly negatively correlated with the amount of ^{14}C recovered as $^{14}CO_2$ (Fig. S4; $P < 0.001$). This supports the notion that ^{14}C-glucose is biotically removed from the soil. Note that only a maximum of 60% of the ^{14}C could be recovered as $^{14}CO_2$ even though most had been removed from soil solution. As the remainder was not recovered from the soil with a NaCl extract we assume that it has been

immobilized in the soil microbial community (Glanville et al., 2016). This is also supported by the dynamics of $^{14}CO_2$ mineralization which shows a classic 2 phase response (see Glanville et al., 2016 for a mechanistic explanation of this C utilization pattern). As the efficiency of the NaOH traps used to capture $^{14}CO_2$ was >95%, the only other C loss pathways we have not considered are volatile losses (e.g. CH_4, VOCs), however, there is no evidence available to support this being a major flux.

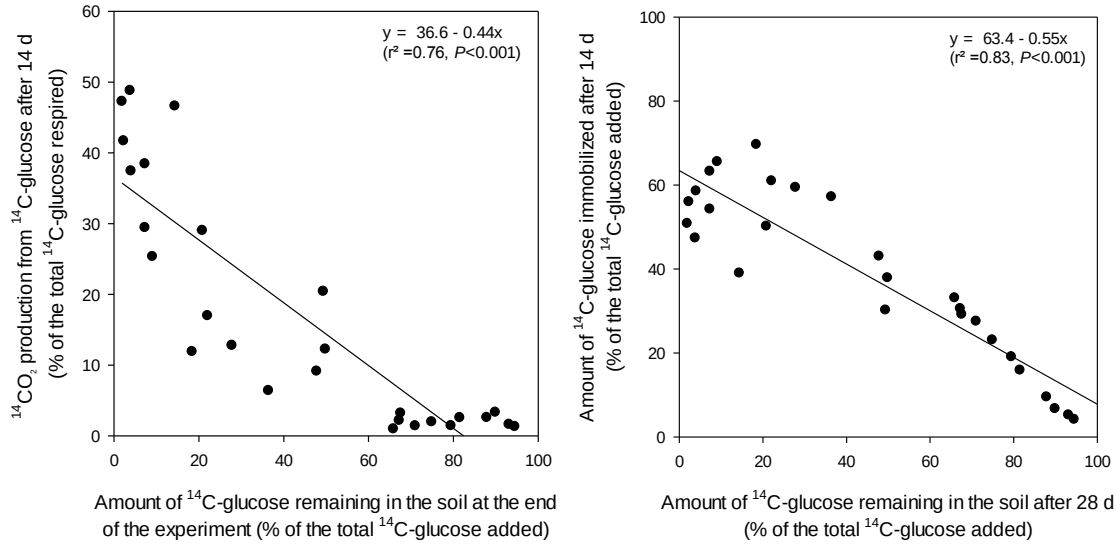

Fig. S4. Relationship between the amount of ^{14}C-glucose remaining in the soil and the amount of the ^{14}C-glucose either respired as $^{14}CO_2$ (left hand panel) or immobilized (right hand panel) by the end of the incubation period across all the samples used in the study (data shown for the wet soil treatment only). The line represents the fitting of a linear regression equation to the experimental data.

S6.2. Relationship between the mineralization of ^{14}C-glucose and ^{14}C-labelled plant material

A good positive linear relationship was apparent between the initial rate of mineralization of the ^{14}C-glucose and ^{14}C-labelled plant material (Fig. S5; $P < 0.001$). No significant relationship, however, was apparent between the two C substrates for the hyper-arid treatment ($P = 0.658$; data not presented).

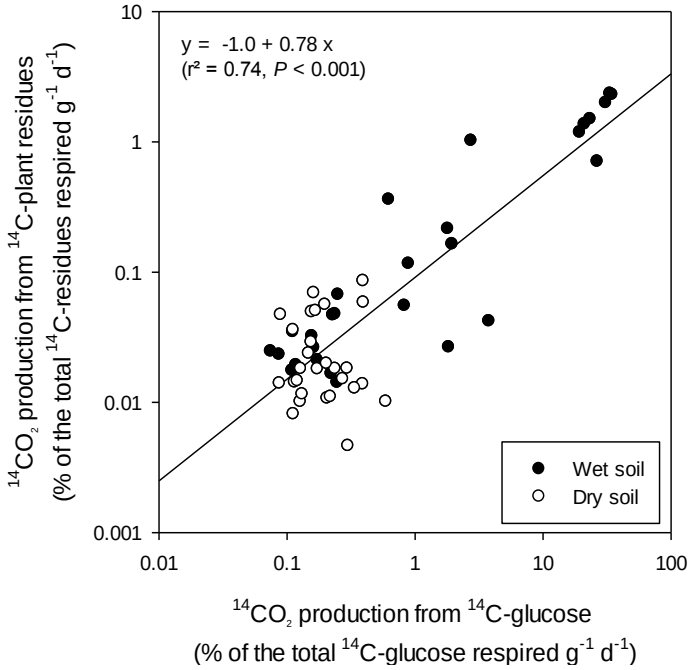

Fig. S5. Relationship between the initial amount of $^{14}CO_2$ produced from ^{14}C-glucose and ^{14}C-plant material across all the different soils. The line represents the fitting of a linear regression equation to the experimental data.

S7. Mineralization of ^{14}C-labelled C substrates as a function of soil depth

S7.1. ^{14}C-labeleld glucose mineralization

Multiple soil depths were sampled at the semi-arid (Paposo) and hyper-arid (Yungay) field sites, but not for the arid sites. At Paposo, soil was sampled at depths of 10-20, 20-40, 40-60, 60-80, 80-100 and 180-200 cm, while at Yungay samples were taken at 20-40 and 120-140 cm. The results for the mineralization of ^{14}C-glucose in the two soil profiles under the three different moisture regimes are presented in Figure S6. As occurred for the surface soils, the rate of mineralization in the subsoils from both profiles followed the series *wet* > *humid* > *hyper-dry*. Generally, the rate of substrate mineralization tended to decline with soil depth. The lower mineralization rate directly at the soil surface probably reflects the lower microbial biomass in the surface layer which is subject to excessive UV radiation (Cockell et al., 2008; Vitek et al., 2010), while at depth it probably reflects the lack of water to support life, rather

than a lack of labile C. This is supported by previous work that has shown significant xeropreservation of organic C at depth. In some cases, the C was deposited between 40,000 and 2 million years ago and still remains unaltered (Wilhelm et al., 2017). The lack of available water at depth is also in alignment with Azua-Bustos et al. (2015) who found that the mean atmospheric relative humidity in the hyper-arid region was 17.3%, and that the relative humidity of the underlying soils remained at a constant 14% down to 1 m. It is clear from both soil profiles, however, that microbial activity is present at depths beyond 1 m. At the hyper-arid site it is unlikely that rainfall events will ever allow free water to reach these depths. Our results do suggest, however, that in comparison to the surface soils, there is a distinct lag phase in $^{14}CO_2$ evolution in subsoils from the semi-arid soil. This suggests that the soil microbial population is low and grows relatively rapidly (i.e. within 48 h) in response to C addition. The apparent plateau in $^{14}CO_2$ production in the wet semi-arid soils suggested that all the glucose was utilised within 7 d. This was supported by the extractions at the end of the incubation period which showed relatively low amounts of ^{14}C-glucose remaining in the soil. Although glucose was mineralized at depth in the hyper-arid soil, no lag phase was seen and the rates of mineralization were very low. This suggests that these organisms are slow growing in comparison to those from the semi-arid site.

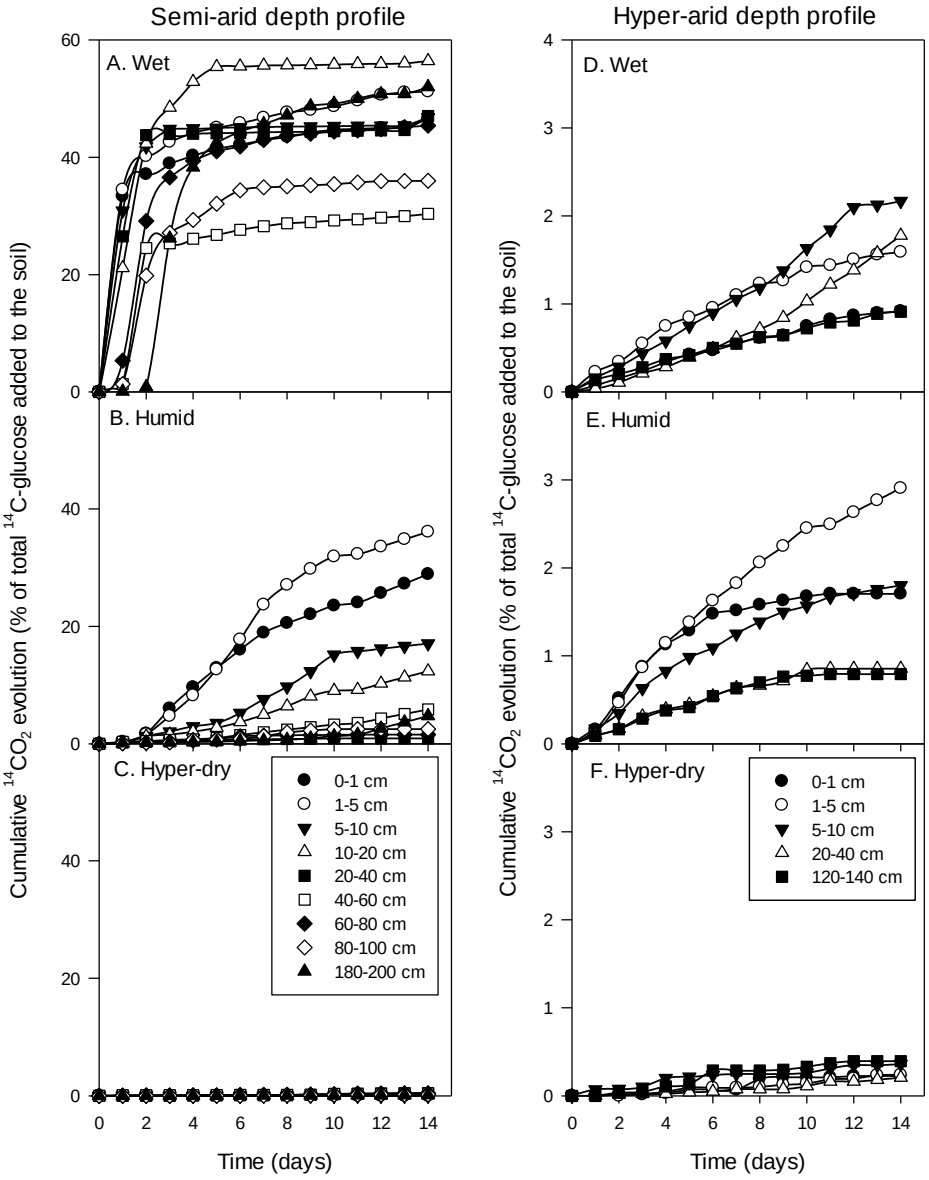

Fig. S6. Temporal dynamics of ^{14}C-glucose mineralization at different depths in a semi-arid (Panels A-C) and hyper-arid (Panels D-F) soil profile from the Atacama Desert under three contrasting moisture regimes (wet, humid and hyper-dry). Note the different y-axis scales for the semi-arid and hyper-arid sites. The legend is the same for all grouped panels.

S7.2. ^{14}C-labeled plant material mineralization

The results for the mineralization of the ^{14}C-plant material in the two soil depth profiles under the three different moisture regimes are presented in Figure S7. Overall, the rate of mineralization in subsoils also showed the trend *wet* > *humid* > *hyper-arid* and tended to decrease with depth. Of note is the longer lag phase in mineralization, particularly in the semi-arid soil. In the semi-arid soil the lag phase lasted ca. 3-5 days in the *wet* conditions and ca. 6-

9 d in the *humid* conditions, while no end to the lag phase was apparent in the *hyper-dry* treatment. The lag phase was longer in the hyper-arid soil and lasted ca. 5-8 days in the *wet* conditions and ca. 6-13 d under the *humid* conditions.

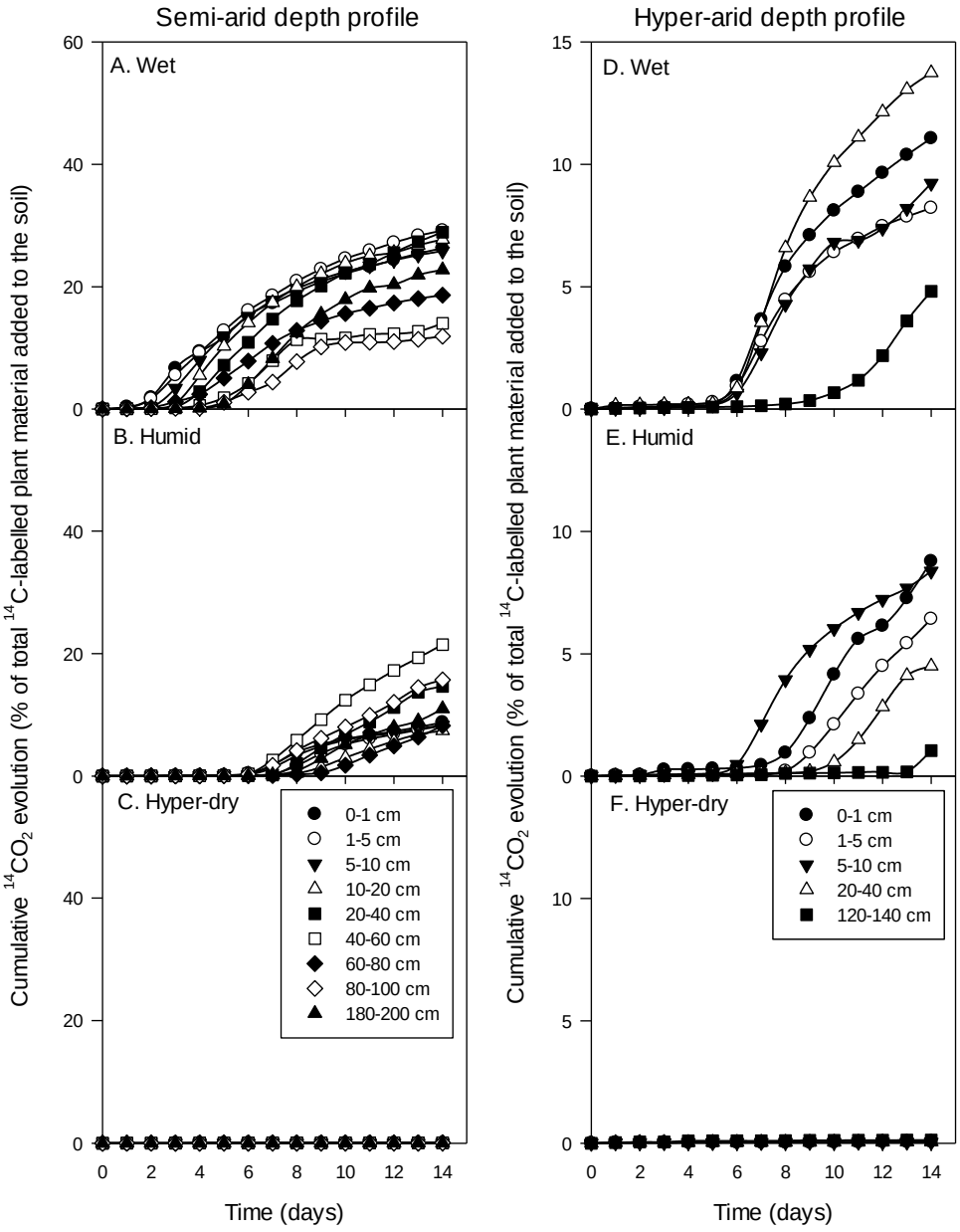

Fig. S7. Temporal dynamics of the mineralization of ^{14}C-labelled plant material at different depths in a semi-arid (Panels A-C) and hyper-arid (Panels D-F) soil profile from the Atacama Desert under three contrasting moisture regimes (wet, humid and hyper-dry). Note the different y-axis scales for the semi-arid and hyper-arid sites. The legend is the same for all grouped panels.

S7.3. Relationship between microbial biomass and substrate mineralization with depth

Estimates of soil microbial biomass using the standard chloroform fumigation-extraction technique of Jörgensen and Müeller (1996) proved unsuccessful. This was due to the low amount of biomass present in the soil which resulted in very small (sometimes negative) differences between the fumigated and unfumigated controls. However, bacterial numbers were estimated by plating out soil extracts on nutrient-rich nutrient broth (NB) media (which favours enumeration of fast growing species) and the nutrient-poor R2A media (which favours the enumeration of slower growing bacteria). Cycloheximide was used in the media to prevent fungal growth. Further details of the methods can be obtained from Claudia Knieff, University of Bonn. We acknowledge that many of the organisms in these soils may not be culturable by these methods. The results for Paposo where we had 9 different soil depths are shown in Table S3. A linear regression analysis of this microbial count data against the initial rate of ^{14}C-glucose and ^{14}C-plant material mineralization for the three different moisture regimes was undertaken (Table S4). The data revealed many good relationships between the number of culturable organisms in soil and the rate of C substrate mineralization. The only poor relationship was with the rate of glucose use under the hyper-dry conditions. No regression analysis was performed for the Yungay profile due to the insufficient number of depth points.

Table S3. Bacterial numbers versus soil depth at the Paposo soil profile (Claudia Knieff, unpublished dataset).

Soil depth	NB medium $\log_{10}$ CFU g^{-1} soil	R2A medium $\log_{10}$ CFU g^{-1} soil
0-1 cm	5.61	6.75
1-5 cm	5.73	6.38
5-10 cm	5.71	6.33
10-20 cm	5.53	5.61
20-40 cm	5.07	5.65
40-60 cm	4.95	5.35
60-80 cm	4.65	5.30
80-100 cm	4.31	5.07
180-200 cm	2.64	4.85

Table S4. Relationship (r^2 linear regression coefficient values) between bacterial numbers enumerated using two different nutrient media (NB and R2A) and the rate of ^{14}C substrate mineralization at different depths in the Paposo soil profile. *, ** and *** indicated a significant relationship at the $P < 0.05$, $P < 0.01$ and $P < 0.001$ level respectively while *NS* indicates no significant relationship ($P > 0.05$).

Substrate type	Moisture regime	Media type	
		NB media	R2A media
^{14}C-glucose	Wet	0.79^{***}	0.52^{*}
	Humid	0.59^{*}	0.84^{***}
	Hyper-dry	0.01^{NS}	0.01^{NS}
^{14}C plant material	Wet	0.31^{NS}	0.88^{***}
	Humid	0.46^{*}	0.16^{NS}
	Hyper-dry	0.81^{***}	0.89^{***}

S8. Relationship between culturable microbial numbers and mineralization rate

Following the same methodology in Section S7, we also compared the initial rate of ^{14}C-susbtrate mineralization with culturable bacteria in the topsoils. It was not possible to obtain reliable count data for all the hyper-arid sites and therefore some data points were missing from the analysis. Overall, however, it was clear that bacterial counts followed the trend *semi-arid* > *arid* > *hyper-arid* (data not presented in this study). Overall, good relationships were seen between mineralization rate and bacterial counts across the topsoils (Table S5).

Table S5. Relationship (r^2 linear regression coefficient values) between bacterial numbers enumerated using two different nutrient media (NB and R2A) and the rate of ^{14}C substrate mineralization in all the surface soils across the semi-arid, arid and hyper-arid sites. *, ** and *** indicated a significant relationship at the $P < 0.05$, $P < 0.01$ and $P < 0.001$ level respectively while *NS* indicates no significant relationship ($P > 0.05$).

Substrate type	Moisture regime	Media type	
		NB media	R2A media
^{14}C-glucose	Wet	0.69^{***}	0.62^{***}
	Humid	0.52^{*}	0.69^{***}
	Hyper-dry	0.01^{NS}	0.01^{NS}
^{14}C plant material	Wet	0.58^{***}	0.86^{***}
	Humid	0.23^{*}	0.01^{NS}
	Hyper-dry	0.45^{**}	0.81^{***}

S9. Average mineralization rates across all the sites used in the study

We calculated the average C substrate mineralization rates across all the sites (semi-arid, arid and hyper-arid) used in the study to provide an overall average for the region (Fig. S8). The difference between the initial rate of mineralization of the glucose and plant material can clearly be seen from these plots. In addition, the initial lag phase in the use of the ^{14}C-labelled plant material can easily be observed. The initial rates (0-48 h) of substrate use across all samples is presented in Table S6. For ^{14}C-glucose, this shows a ca. 10- to 20-fold increase in rate between the wet, humid and hyper-arid treatments. Although the same trend was observed for the ^{14}C-labelled plant material, the differences were only 2-5-fold between moisture treatments.

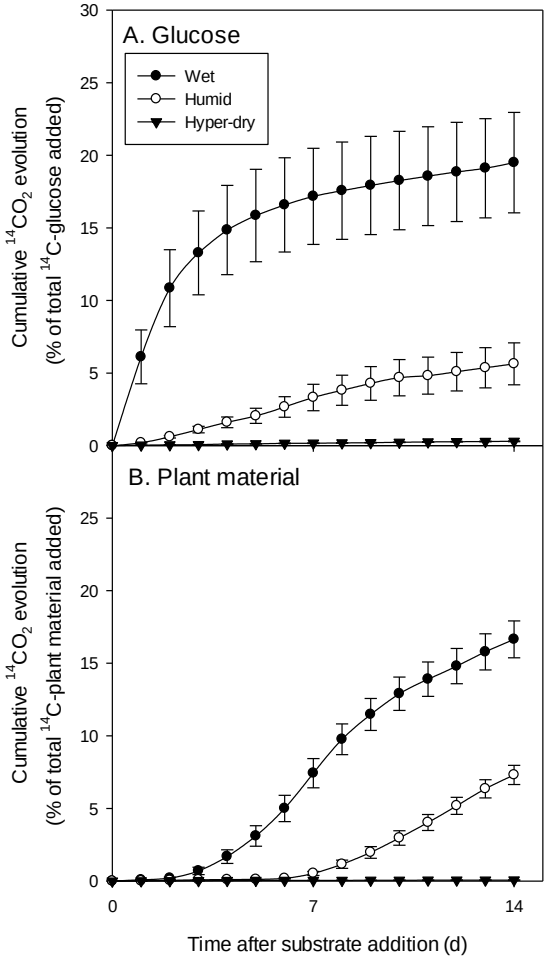

Fig. S8. Temporal dynamics of the mineralization of ^{14}C-labelled glucose and plant material across all samples used in the study under three contrasting moisture regimes (wet, humid and hyper-dry).

Table S6. Initial rate of ^{14}C-labelled substrate mineralization across all samples (semi-arid, arid and hyper-arid) at the three contrasting moisture regimes. Values represent means ± SEM.

Moisture regime	^{14}C-glucose (% g^{-1} d^{-1})	^{14}C-plant material (% g^{-1} d^{-1})
Wet	5.42 ± 1.32	0.108 ± 0.034
Humid	0.31 ± 0.04	0.024 ± 0.005
Hyper-dry	0.03 ± 0.01	0.011 ± 0.002

Section S10. Moisture sorption to the soil in the humid treatment

To assess the rate of moisture uptake by the soil and the potential activation of the soil microbial community, we measured the weight gain in nine soils (3 each from the semi-arid, arid and hyper-arid treatments) after being placed in a humid treatment. Briefly, the experiment was identical to that in the main manuscript, except that the samples were pre-equilibrated over Drierite® for 7 d and weighed (±0.00001 g) over the incubation period (14 d, 20°C). All soils showed a tri-phasic response in water sorption. There was an initial rapid uptake of water (0-6 h), followed by a second slower linear phase followed by a third phase when the soil was at quasi-equilibrium with the surrounding water vapour (Fig. S9). Water adsorption is directly related to relative humidity (Schneider and Goss, 2012; Arthur et al., 2015) and the high humidity maintained in our samples would have promoted maximal water uptake by the soil (Leao and Tuller, 2014; Arthur et al., 2014). The equilibrium values reported for our soils (ca. 30 mg g^{-1}) are within the range reported for other soils (10-100 mg g^{-1}), but tended to be at the lower end suggesting they have a low specific surface area (Grismer, 1987; Leao and Tuller, 2014; Arthur et al., 2014ab; Arthur et al., 2015). Although not measured, it should be noted that the plant material can also readily adsorb water from a humid atmosphere and wick moisture from soil (Stuart et al., 2015; Wolf et al., 2016). Both these processes will have facilitated activation of the endemic microbial community in the plant residues and the diffusive loss of solutes from the residues into the soil (Dirks et al., 2010).

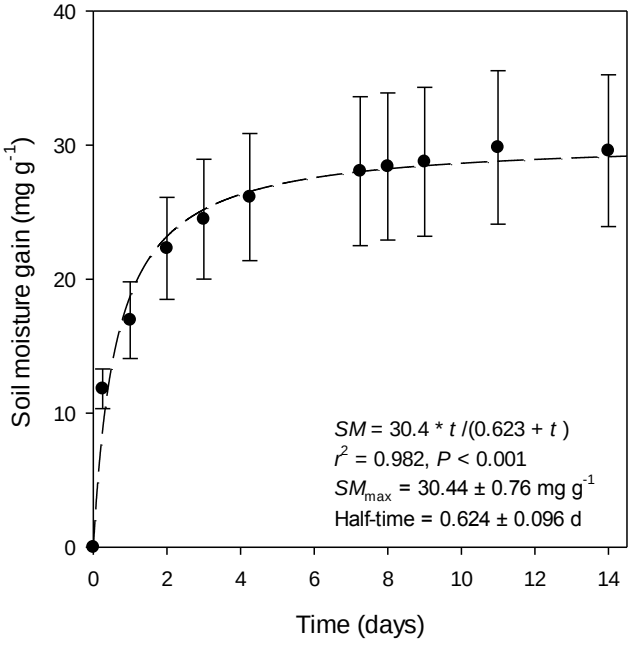

Fig. S9. Temporal dynamics of water vapour sorption onto soils from the Atacama Desert when exposed to a humid atmosphere (RH >80%). Values represent means ± SEM, n = 9. The dotted line represents the fit of a hyperbolic function to the experimental data. In the equation, SM is soil moisture, SM_{max} is the maximum moisture gain under the experimental conditions, t is time and the half-time is the time taken to reach half the maximal water adsorption.
9.

Section S11. Contributions to the manuscript

The concept for this study originated from DLJ, RB and PWH. The soil samples were collected by RB, EK, EL and CK. The main radiotracer experiments were undertaken by SOA and DLJ while the microbial cell count study was undertaken by CK. The data analysis was performed by DLJ and SOA. The manuscript was drafted by DLJ and RB and further edited by EK, CK, PWH and EL prior to submission.

References

Acuna, E.A.A., Pastenes, V.C., Villalobos, G.L., 2017. Carbon sequestration and photosynthesis in newly established turfgrass cover in Central Chile. Agronomy Journal 109, 397-40.

Aggarwal, R.K., Praveenkumar, 1994. Availability and management of nitrogen in soils of arid ecosystem. Annals of Arid Zone 33, 1-18.

Agnew, S.F., Reynolds, J.G., Johnston, C.T., 2012. Predicting water activity for complex wastes with solvation cluster equilibria (SCE). Proceedings of the Wste Management Symposia (WM2012 Conference), February 26th - March 1st, 2012, Phoenix, AZ, USA.

An, Y., Wang, D., Wu, C., 2014. Ion-exchange between $Na_2Ti_3O_7$ and $H_2Ti_3O_7$ nanosheets at different pH levels: An experimental and first-Principles study. Physica E-Low-Dimensional Systems & Nanostructures 60, 210-213.

Arthur, E., Tuller, M., Moldrup, P., de Jonge, L.W., 2014a. Rapid and fully automated measurement of water vapor sorption isotherms: New opportunities for vadose zone research. Vadose Zone Journal 13, doi: 10.2136/vzj2013.10.0185.

Arthur, E., Tuller, M., Moldrup, P., de Jonge, L.W., 2014b. Evaluation of a fully automated analyzer for rapid measurement of water vapor sorption isotherms for applications in soil science. Soil Science Society of America Journal 78, 754-760.

Arthur, E., Tuller, M., Moldrup, P., de Jonge, L.W., 2015. Effects of biochar and manure amendments on water vapor sorption in a sandy loam soil. Geoderma 243, 175-182.

Azua-Bustos, A., Caro-Lara, L., Vicuña, R., 2015. Discovery and microbial content of the driest site of the hyperarid Atacama Desert, Chile. Environmental Microbiology Reports 7, 388-394.

Barros, N., Feijoo, S., Salgado, J., Ramajo, B., Garcia, J.R., Hansen, L.D., 2008. The dry limit of microbial life in the Atacama Desert revealed by calorimetric approaches. Engineering in Life Sciences 8, 477-486.

Bennett, B.D., Kimball, E.H., Gao, M., Osterhout, R., van Dien, S.J., Rabinowitz, J.D., 2009. Absolute metabolite concentrations and implied enzyme active site occupancy in *Escherichia coli*. Nature Chemical Biology 5, 593-599.

Berger, I.A., Cooke, R.U., 1997. The origin and distribution of salts on alluvial fans in the Atacama Desert, northern Chile. Earth Surface Processes and Landforms 22, 581-600.

Campillo, R., Urquiaga, S., Undurraga, P., Pino, I., Boddey, R.M., 2005. Strategies to optimise biological nitrogen fixation in legume/grass pastures in the southern region of Chile. Plant and Soil 273, 57-67.

Cockell, C.S., Mckay, C.P., Warren-Rhodes, K., Horneck, G., 2008. Ultraviolet radiation-induced limitation to epilithic microbial growth in and deserts - Dosimetric experiments in the hyperarid core of the Atacama Desert. Journal of Photochemistry and Photobiology B-Biology 90, 79-87.

Cordero, R.R., Seckmeyer, G., Damiani, A., Riechelmann, S., Rayas, J., Labbe, F., Laroze, D., 2014. The world's highest levels of surface UV. Photochemical and Photobiological Sciences 13, 70-81.

Davila, A.F., Hawes, I., Araya, J.G., Gelsinger, D.R., DiRuggiero, J., Ascaso, C., Osano, A., Wierzchos, J., 2015. In situ metabolism in halite endolithic microbial communities of the hyperarid Atacama Desert. Frontiers in Microbiology 6, 1035.

Dirks, I., Navon, Y., Kanas, D., Dumbur, R., Grunzweig, J.M., 2010. Atmospheric water vapor as driver of litter decomposition in Mediterranean shrubland and grassland during rainless seasons. Global Change Biology 16, 2799-2812.

Domisch, T., Finer L., Karsisto, M., Laiho, R., Laine1, J., 1998. Relocation of carbon from decaying litter in drained peat soils. Soil Biology & Biochemistry 30, 1529-1536.

Ehleringer, J.R., Rundel, P.W., Palma, B., Mooney, H.A., 1998. Carbon isotope ratios of Atacama Desert plants reflect hyperaridity of region in northern Chile. Revista Chilena de Historia Natural 71, 79-86

Ekschmitt, K., Kandeler, E., Poll, C., Brune, A., Buscot, F., Friedrich, M., Gleixner, G., Hartmann, A., Kästner, M., Marhan, S., Miltner, A., Scheu, S., Wolters, V., 2008. Soil-

carbon preservation through habitat constraints and biological limitations on decomposer activity. Journal of Plant Nutrition and Soil Science 171, 27-35.

Evenstar, L.A., Hartley, A.J., Stuart, F.M., Mather, A.E., Rice, C.M., Chong, G., 2009. Multiphase development of the Atacama Planation Surface recorded by cosmogenic 3He exposure ages: implications for uplift and Cenozoic climate change in western South America. Geology 37, 27-30.

Ewing, S.A., Sutter, B., Owen, J. Nishiizumi, K., Sharp, W., Cliff, S.S., Perry, K., Dietrich, W., McKay, C.P., Amundson, R., 2006. A threshold in soil formation at Earth's arid-hyperarid transition. Geochimica Cosmochimica Acta 70, 5293-5322.

Ewing, S.A., Macalady, J., Warren-Rhodes, K., McKay, C., Amundson, R., 2008. Changes in the soil C cycle at the arid-hyperarid transition in the Atacama Desert. Journal of Geophysical Research 113, G02S90.

Faria, M., Hotchkiss, J.H., Wraight, S.P., 2012. Application of modified atmosphere packaging (gas flushing and active packaging) for extending the shelf life of *Beauveria bassiana* conidia at high temperatures. Biological Control 61, 78-88.

Fletcher, L.E., Valdivia-Silva, J.E., Perez-Montano, S., Condori-Apaza, R., Conley, C.A., McKay, C. 2012. Variability of organic material in surface horizons of the hyper-arid Mars-like soils of the Atacama Desert. Advances in Space Science 49, 271-279.

Garreaud, R., Barichivich, J., Christie, D.A., Maldonado, A., 2008. Interannual variability of the coastal fog at Fray Jorge relict forests in semiarid Chile. Journal of Geophysical Research 113, G04011.

Glanville, H., Hill, P.W., Schnepf, A., Oburger, E., Jones, D.L., 2016. Combined use of empirical data and mathematical modelling to better estimate the microbial turnover of isotopically labelled carbon substrates in soil. Soil Biology & Biochemistry 94, 154-168.

Grant, W.D., 2004. Life at low water activity. Philosophical Transactions of the Royal Society of London. Series B, Biological Sciences 359, 1249-1267.

Grismer, M.E., 1987. Water-vapor adsorption and specific surface. Soil Science 144, 233-236.

Houston, J., Hartley, A.J., 2003. The central Andean west-slope rainshadow and its potential contribution to the origin of hyper-aridity in the Atacama Desert. International Journal of Climatology 23, 1453-1464.

Jörgensen, R.G., Müeller, T., 1996. The fumigation-extraction method to estimate soil microbial biomass: Calibration of the k_{EN} value. Soil Biology & Biochemistry 28, 33-37.

Jones, D.L., Darrah, P.R., 1994. Simple method for ^{14}C labeling root material for use in root decomposition studies. Communications in Soil Science and Plant Analysis 25, 2737-2743.

Jones, D.L., Darrah, P.R., 1996. Re-sorption of organic compounds by roots of *Zea mays* L. and its consequences in the rhizosphere. 3. Characteristics of sugar influx and efflux. Plant and Soil 178, 153-160.

Jones, D.L., Willett, V.B., 2006. Experimental evaluation of methods to quantify dissolved organic nitrogen (DON) and dissolved organic carbon (DOC) in soil. Soil Biology & Biochemistry 38, 991-999.

Kuzyakov, Y., Jones, D.L., 2006. Glucose uptake by maize roots and its transformation in the rhizosphere. Soil Biology & Biochemistry 38, 851-860.

Leao, T.P., Tuller, M., 2014. Relating soil specific surface area, water film thickness, and water vapor adsorption. Water Resources Research 50, 7873-7885.

Lynch, R.C., Darcy, J.L., Kane, N.C., Nemergut, D.R., Schmidt, S.K., 2014. Metagenomic evidence for metabolism of trace atmospheric gases by high-elevation desert Actinobacteria. Frontiers in Microbiology 5, 698.

McKay, C.P., Fridmann, I., Gómez-Silva, B., Cáceres-Villanueva, L., Anderson, D.T., Landheim, R., 2003. Temperature and moisture conditions for life in the extreme arid region of the Atacama Desert: four years of observation including El Nino of 1997-1998. Astrobiology 3, 393-406.

McKay, C.P., 2014. Requirements and limits for life in the context of exoplanets. Proceedings of the National Academy of Sciences 111, 12628-12633.

Moorhead, D.L., Sinsabaugh, R.L., 2006. A theoretical model of litter decay and microbial interaction. Ecological Monographs 76, 151-174.

Patzelt, D. J., Hodač, L., Friedl, T., Pietrasiak, N., Johansen, J.R., 2014. Biodiversity of soil cyanobacteria in the hyper-arid Atacama Desert, Chile. Journal of Phycology 50, 698-710.

Quinn, R.C., Ehrenfreund, P., Grunthaner, F.J., Taylor, C.L., Zent, A.P., 2007. Decomposition of aqueous organic compounds in the Atacama Desert and in Martian soils. Journal of Geophysical Research-Biogeosciences 112, G04S18.

Reis, J., Sitaula, R., Bhowmick, S., 2009 Water activity and glass transition temperatures of disaccharide based buffers for desiccation preservation of biologics. Journal of Biomedical Science and Engineering 2, 594-605.

Robinson, C.K., Wierzchos, J., Black, C., Crits-Christoph, A., Ma, B., Ravel, J., Ascaso, C., Artieda, O., Valea, S., Roldán, M., Gómez-Silva, B. and DiRuggiero, J., 2015. Microbial diversity and the presence of algae in halite endolithic communities are correlated to atmospheric moisture in the hyper-arid zone of the Atacama Desert. Environmental Microbiology 17, 299-315.

Rondanelli, R., Molina, A., Falvey, M., 2015. The Atacama surface solar maximum. Bulletin of the American Meteorological Society 96, 405-418.

Rundel, P.W., 1978. Ecological relationships of desert fog zone lichens. The Bryologist 81, 277-293.

Rundel, P.W., Mahu, M., 1976. Community structure and diversity in a coastal fog desert in Northern Chile. Flora 165, 493-505.

Rundel, P.W., Dillon, M.O., Palma, B., Mooney, H.A., Gulmon, S.L., Ehleringer, J.R., 1991. The phytogeography and ecology of the coastal Atacama and Peruvian deserts. A Journal of Systematic and Evolutionary Botany 13, Article 2.

Schneider, M., Goss, K., 2012. Prediction of the water sorption isotherm in air dry soils. Geoderma 170, 64-69.

Stuart, T., McCall, R.D., Sharma, H.S.S., Lyons, G., 2015. Modelling of wicking and moisture interactions of flax and viscose fibres. Carbohydrate Polymers 123, 359-368.

Sutter, B., Dalton, J.B., Ewing, S.A., Amundson, R., McKay, C.P., 2007. Terrestrial analogs for interpretation of infrared spectra from the Martian surface and subsurface: Sulfate, nitrate, carbonate, and phyllosilicate-bearing Atacama Desert soils. Journal of Geophysical Research-Biogeosciences 112, G04S10.

Teusink, B., Diderich, J.A., Westerhoff, H.V., van Dam, K., Walsh, M.C., 1998. Intracellular glucose concentration in derepressed yeast cells consuming glucose is high enough to reduce the glucose transport rate by 50%. Journal of Bacteriology 180, 556-562.

Vitek, P., Edwards, H.G.M., Jehlicka, J., Ascaso, C., De los Rios, A., Valea, S., Jorge-Villar, S.E., Davila, A.F., Wierzchos, J., 2010. Microbial colonization of halite from the hyper-arid Atacama Desert studied by Raman spectroscopy. Philosophical Transactions of the Royal Society A-Mathematical Physical and Engineering Sciences 368, 3205-3221.

Vrede, K., Heldal, M., Norland, S., Bratbak, G., 2002. Elemental composition (C, N, P) and cell volume of exponentially growing and nutrient-limited bacterioplankton. Applied and Environmental Microbiology 68, 2965-2971.

Wang, F., Ge, W.S., Luo, H., Seo, J.H., Michalski, G., 2016. Oxygen-17 anomaly in soil nitrate: A new precipitation proxy for desert landscapes. Earth and Planetary Science Letters 438, 103-111.

Warren-Rhodes, K.A., Rhodes, K.L., Pointing, S.B., Ewing, S.A., Lacap, D.C., Gómez-Silva, B., Amundson, R., Friedmann, E.I., McKay, C.P., 2006. Hypolithic cyanobacteria, dry limit of photosynthesis, and microbial ecology in the hyperarid Atacama Desert. Microbial Ecology 52, 389-398.

Wierzchos, K., Cancilla, J.C., Torrecilla, J.S., Díaz-Rodríguez, P., Davila, A.F., Ascaso, C., Nienow, J., McKay, C., PWierzchos, J., 2015. Application of artificial neural networks as a tool for moisture prediction in microbially colonized halite in the Atacama Desert. Journal of Geophysical Research Biogeosciences 120, 1018-1024.

Wierzchos, J., Camara, B., De Los Rios, A., Davila, A.F., Almazo, I.M.S., Artieda, O., Wierzchos, K., Gomez-Silva, B., Mckay, C., Ascaso, C., 2011. Microbial colonization of Ca-sulfate crusts in the hyperarid core of the Atacama Desert: implications for the search for life on Mars. Geobiology 9, 44-60.

Wilhelm, M.B., Davila, A.F., Eigenbrode, J.L., Parenteau, M.N., Jahnke, L.L., Liu, X.L., Summons, R.E., Wray, J.J., Stamos, B.N., O'Reilly, S.S., Williams, A., 2017. Xeropreservation of functionalized lipid biomarkers in hyperarid soils in the Atacama Desert. Organic Geochemistry 103, 97-104.

Wolf, C., Guillard, V., Angellier-Coussy, H., Silva, G.G.D., Gontard, N., 2016. Water vapor sorption and diffusion in wheat straw particles and their impact on the mass transfer properties of biocomposites. Journal of Applied Polymer Science 133, Article 43329.